Effects of Biaxial Loading on Three-Dimensional Crack Front Fields

Huang Yuan*

Abstract

In this paper we studied the crack front fields under small-scale yielding conditions. Effects of the out-of-plane fields in three-dimensional cases were emphasised. The stress fields develop towards the plane stress with increasing applied loads. So the specimen thickness plays a key role in characterisations of the three-dimensional crack-tip fields. The out-of-plane constraints are a decreasing function of the applied loads. The second terms in the three-dimensional stress fields are dependent on distance to the tip and to the free edge-surface of the specimen. It was shown that the stress triaxiality at the crack front is substantially a linear function of Q. Q characterises variations of the stress triaxiality at the three-dimensional crack front fields. Our results confirmed that the normalised hydrostatic stress over Mises stress is not uniquely correlated with the stress triaxiality at the tip front.

1 Introduction

Three-dimensional crack front fields in elastic-plastic materials have been extensively studied since several years [1, 2, 3, 4]. Whereas most analyses concentrated on surface-cracked specimens, e.g. in [2, 3], Nakamura and Parks [1] performed detailed finite-element calculations in the crack front fields containing substantial plane stress components. It has been shown that the crack front field is dominated by the plane strain solution only when the applied loads are vanishingly small. The whole field is characterised by the plane stress solution if the size of the plastic zone is larger than 1.5 times of the plate thickness. This result implies that in many experiments using the conventional cracked specimens effects of the plane stress field are not negligible. Parks [5] reviewed the results of two different cracked geometries, which were reported in [1, 3], and concluded that the crack front fields deviated from the HRR-

*Research Center Neumünster, NU TECH GmbH, 24536 Neumünster, Germany

or SSY-type constraint significantly. It is desirable to extend detailed finite element analysis, as Hancock and co-workers [7, 8] have demonstrated for the two-parameter plane strain, to three-dimensional local fields.

Quantification of the local constraint effects at the crack tip have been intensively studied recently [7, 8, 9, 10, 17]. Most results are restricted to two-dimensional plane strain cases and partially in surface-cracked panels [18], in which the crack front fields seem near to plane strain. In these cases variations of the out-of-plane stress, σ_{zz}, can be represented by the in-plane normal stresses through the material constitutive equations. So the constraint problem dealt with is practically simplified to investigation of the in-plane fields. Further discussions in more general three-dimensional crack fields are extended to what and how the second-parameter for crack-tip fields should be, especially when the out-of-plane stress fields cannot be characterised by the in-plane stresses. Is it T, [6, 7, 8], Q [9, 10, 17] or even the normalised stress triaxiality (σ_m/σ_e) directly [2, 12]? Each parameter has its different physical background and causes advantages on this side and drawbacks on the other side [14].

In the present paper we have discussed quantification of the constraint effects in Ramberg-Osgood materials under small-scale yielding conditions. The small-scale yielding denotes such cases that the size of the plastic zone is much smaller than a characteristic dimension of the specimen ($r_r/t << 1$). The in-plane boundaries of the specimens do not affect the crack-tip fields. The efforts were devoted to investigate effects of the specimen thickness coupled with the biaxial loading. More general discussions including general yielding in finite cracked geometry will be reported in a separate paper.

2 Finite Element Model

The geometry considered in this section is analogous to that introduced by Nakamura and Parks [1]. We image a plate which under arbitrary remote loading contains an annular region where the local deformation field may be essentially characterised by a scalable eigensolution (the HRR-solution), which is independent of the aspects of in-plane geometry and loading. A circular disc containing the crack tip in a large plate was removed, modelling the near tip region with the modified boundary layer formulation (Fig. 1). The biaxial loads are applied through the transverse T-stress. The straight crack front is located at the centre of the disc along the z-axis $(x, y = 0)$. Only a quarter of the disc $(0 < \theta < \pi, 0 < z/t < 1)$ was modelled. The radial extent of the disc was $r_{max} = 20t$, where the in-plane K displacement boundary conditions

$$u_\alpha = \frac{K}{E} g_\alpha(\theta, \nu)\sqrt{\frac{r}{2\pi}} + \frac{T}{E} h_\alpha(\theta, \nu) \tag{1}$$

were applied uniformly across the thickness. In the equation E and ν represent Young's modulus and Poisson's ratio, respectively. g_α and h_α are known dimensionless angular functions. The out-of-plane displacement in the remote radius (r_{max}) is distributed linearly along the coordinate z, which corresponds to the plane stress solution [13]. Numerical calculations have shown that the further variations of the remote radius do not change the eigensolution at the three-dimensional crack front. The load is thus characterised by $J = K^2/E$, where J denotes the Rice's J-integral [11]. In the three-dimensional crack analysis the J-integral is generally a function of the thickness coordinate z, the local J-integral. Without additional explanations, J denotes the local J-integral throughout this text. The problem discussed in the present work contains three characteristic dimensions, they are thickness t, the applied load $J/\sigma_0\epsilon_0$ and the transverse load represented through $\tau = T/\sigma_0$. The length dimensions of a plate can be normalised with these scales [1].

Our numerical calculations have shown furthermore that the stress field characterised by the plane strain or plane stress may be obtained under suitable biaxiality ratio K/T. In this work we have classified two different stress fields: One with very small plastic zone size in comparing with the plate thickness ($r_p/t < 0.1$) corresponds a field dominated by the plane strain solution, and the other has a plastic zone dimension corresponding the thickness ($r_p/t > 0.5$) and is increasingly effected by the plane stress solution from the edge-surface ($z/t = 1$). The analysis of the boundary layer formulation with T-stress in the range $-1 < \tau < 1$ is considered. Note that the size of the plastic zone is sensitive to the loading path, K/T, in general. Only for some values of K/T the small-scale yielding solution can be obtained up to $|\tau| = 1$. A solution for $|\tau| > 1$ cannot be generated by the boundary layer formulation since small-scale yielding conditions will be violated.

The ABAQUS general-purpose finite element program [15] has been used for the computations. In all finite element calculations the J-integral has been calculated by the virtual crack extension method, which is implemented in ABAQUS. The radial length of the smallest elements is about $10^{-6}a$, where a denotes the crack length which is represented by the remote radius r_{max} in the boundary layer formulation (Fig. 1). The mesh in the radial direction is generated by exponential scaling. The finite element model is constructed using 8-nodal isoparametric elements with 2×2 Gaussian integration. There are 24 elements within the angular region from 0 to π in the crack-tip region. To catch the significant changes of the stress fields near the free edge-surface, 13 elements are spanned along the crack front and the element brick thickness in a potential form. The thickness of the elements near the free edge-surface is about 0.01 of those near the mid-plane. In the present paper, all computations have been performed under deformation plasticity und inifinitesimale strain theory. The stress-strain relation is given through the Ramberg-Osgood model

with a strain-hardening exponent $n = 10$.

3 Results and Discussions

O'Dowd and Shih [9, 10] have examined the characteristics of the high and low stress triaxialities surrounding the finite strain zone and introduced the $J - Q$ annulus in the framework of the J_2-deformation theory of plasticity. In their studies the plane strain solution of the modified boundary layer formulation, $[\sigma_{ij}]^{SSY,T=0}$, was taken as the reference solution. The second term quantifying the relevant stress triaxiality was obtained by subtracting the reference solution scaled by the applied J from the full-field solution, i.e.

$$\sigma_{ij} = \left[\sigma_{ij}\left(\frac{r}{J/\sigma_0}, \theta\right)\right]^{SSY,T=0} + Q\sigma_0\hat{\sigma}_{ij}(r,\theta), \tag{2}$$

where σ_0 denotes the yield stress of the material. Under the J_2-deformation theory of plasticity with Ramberg-Osgood model, O'Dowd and Shih [9, 10] have found the second terms in (2) may be replaced by the Kronecker-delta, which read

$$\sigma_{ij} = \left[\sigma_{ij}\left(\frac{r}{J/\sigma_0}, \theta\right)\right]^{SSY,T=0} + Q\sigma_0\delta_{ij}, \tag{3}$$

in the forward sector ($\theta < \pi/2$), where the dimensionless parameter

$$Q = \frac{\sigma_{\theta\theta} - \sigma_{\theta\theta}^{SSY,T=0}}{\sigma_0} \quad \text{at} \quad \frac{r}{J/\sigma_0} = 2, \theta = 0 \tag{4}$$

defines a measure of the near-tip stress triaxiality, or crack-tip constraint, relative to a reference high triaxiality stress state.

Under plane strain conditions this point has been confirmed by many further numerical investigations. As soon as the crack field deviates from the plane strain solution, the stresses at the crack tip cannot be represented by (3) in general. Plane stress calculations [16] have shown that the hoop stress ahead of the crack-tip is hardly affected by the transverse stress under small-scale yielding conditions. Based on this observation, it is to expect that the crack front fields in three dimensional cracked geometry will be increasingly dependent on the size of the plastic zone around the crack-tip.

This point is confirmed in Figs. 2 and 3, in which the second term of the hoop stress $\sigma_{\theta\theta}$ of Equation (3) is plotted as a function of distance to and the polar angle around the crack tip in the two different load levels classified previously. The stress values are taken from the Gaussian integration points near to the ligament

($\theta = 1.5°$). Note that J/σ_0 is the relevant length scale on the order of CTOD. In two-dimensional cases the curves are independent of the applied K values. The stress and strain distributions with the same T-stress value collapse onto a single curve, when the distance from the tip is normalised by J/σ_0. In the three-dimensional crack front fields, however, the stress curves depend on development of the plastic zone and on the applied loads. The plastic zones for Figs. 2a and 2b are restricted in $r_p < 0.1t$. The transverse stress is limited to $|\tau| < 0.6$. Beyond this value the plastic zone grows quickly. It is clearly seen that the stress fields at both the mid-plane ($z/t = 0.056$) and in the edge-surface ($z/t = 0.996$) contain substantial plane strain components. Variations of the stresses with respect to different transverse T-stress are analogous to the known plane strain solution [9]. Similar features can also be observed in the corresponding angular variations (Figs. 2c and 2d). As applied load intensity K increases, the stress field near the tip develops towards plane stress [1]. Fig. 3 plots the finite element results with a plastic zone in dimension of the plate thickness. It is to see that the crack front fields are dominated by plane stress [16]. Note the characteristics of the crack front fields depends on the relative size of the plastic zone comparing with the plate thickness.

In the plane strain calculations Betegón and Hancock [8] as well as O'Dowd and Shih [9] have demonstrated that the stress fields are practically independent of the positive T-stress. Only the negative T-stress will reduce the hydrostatic stress at the crack tip. Wang [3] has suggested that the plane strain hoop stress with respect to the transverse stress can be expressed through

$$\sigma_{\theta\theta}\left(\frac{r}{J/\sigma_0}, \theta, \tau\right) = \sigma_{\theta\theta}\left(\frac{r}{J/\sigma_0}, \theta, \tau = 0\right) + A\tau + B\tau^2 + C\tau^3, \tag{5}$$

where A, B and C are coefficients depending on the material properties [17]. From (5) Q can be determined through

$$Q = A\tau + B\tau^2 + C\tau^3, \tag{6}$$

Discussions in an engineering material [20] have shown that (5) can only be valid if the crack-tip field is vanishingly affected by the plastic zone development. The coefficients of the equation are not only functions of material properties but also the applied load. This can be observed further in the present work. Fig 4 shows Q evaluated according to (4) as a function of the transverse T-stress in different load levels. In the MBLF, the T-stress is known according to its definition. The plane strain result of the Ramberg-Osgood material with $n = 10$ in the figure is extracted from [17]. Obviously, the curves of the crack front fields increasingly deviate from the plane strain with applied loads. Even in small-scale yielding with $r_p/t < 0.1$ Q differs from the known solution significantly, though the curves can be approximated by a similar polynomial as in (6). This non-unique correlations between T and Q imply

that the $J-T$ description cannot give an accurate estimation of the stress fields in some three-dimensional cases at least.

It has been shown that the three-dimensional crack-tip fields are generally affected by the plate thickness significantly. Only when r_p/t becomes vanishingly small, the crack front fields can be described by the plane strain fields. Then the out-of-plane and the in-plane constraint effects can be treated with $Q-J$ or $T-J$ uniformly. Based on the discussions above, the characterisation of the hydrostatic stress should be a function of the specimen geometry as well as the material properties, that is

$$\sigma_m = \sigma_0 \Omega(Q, r_p/t, \text{Material Properties}). \tag{7}$$

In this expression the stress triaxiality at $r = 2J/\sigma_0$ and $\theta = 0$ is explicitly independent of the applied loads. The Equation (7) is plotted in Fig. 5a for different applied K and T as well as at different z/t. It is interesting to observe that the stress triaxiality at the tip is essentially a linear function of Q. The Equation (7) can be re-written as

$$\frac{\sigma_m}{\sigma_0} = b_1 Q + b_0, \tag{8}$$

where the factors b_0 and b_1 are functions of the cracked geometry and the material properties. Recalling the definition of the Q factor, one may see that b_0 is the triaxiality of the plane strain reference solution. In the present definition (4), it is the plane strain small-scale yielding results with $T = 0$. Our numerical calculations have shown that b_1 depends slightly on the geometry of the specimens. In the present work, b_1 approximately equals 1. This results have been further confirmed in other conventional cracked geometries which have been examined in [14, 20]. Q generally represents the local difference of the stress triaxiality in the three-dimensional crack fields. Recalling the definition of Q and the variation of the second term in the crack-tip fields (Figs. 2 and 3), we see that the Q value only locally represents the stress triaxiality at $r/(J/\sigma_0) = 2$ and $\theta = 0$. Q may not give a general description of the whole stress field at the crack front.

Fig. 5b displays the correlation between Q and the normalised hydrostatic stress σ_m/σ_e [2]. The normalised hydrostatic stress was suggested to characterise the constraint effects in analogy to the known continuum damage model for ductile materials. The result in Fig. 5b shows that the parameter σ_m/σ_e is not equivalent to Q.

4 Concluding Remarks

With three-dimensional modified boundary layer formulation it has been shown that the crack front fields are not only affected by the transverse T-stresses but also by the

applied J-integral. Only when the applied J-integral becomes vanishingly small, the stress can be described by the plane strain solution. Otherwise, the size of the plastic zone is a characteristic parameter for the three-dimensional stress fields. For the cases with $r_p/t > 0.5$, the stress fields contain substantial plane stress components.

In the present three-dimensional analysis, T does not give an accurate description of the stress field. The non-unique correlations between T and Q imply that T cannot provide an accurate estimate of the stress triaxiality at the crack tip. Only when in the low load case the second term of the hoop stress defined in (3) satisfies the assumption introduced under the plane strain conditions in [17]. With the applied loads the second term becomes increasingly dependent on both polar angle and radial distance to the crack front. Although Q linearly depends on the hydrostatic stress σ_m, Q represents variation of the stress triaxiality at $r/(J/\sigma_0) = 2$ and $\theta = 0$ only.

Acknowledgements: The computations reported were performed on an IBM-RISC workstation at GKSS-Research Center Geesthacht, Germany.

References

[1] Nakamura, T. and Parks, D. M. (1990), *Journal of the Mechanics and Physics of Solids*, 38, pp. 787-812

[2] Brocks, W. and Olschewski, J. (1986), *International Journal of Solids and Structures*, Vol. 22, pp. 693-708.

[3] Wang, Y.-Y., (1993) in *Constraint Effects in Fracture, ASTM STP 1171*, American Society for Testing and Materials, Philadelphia, pp. 120-138.

[4] Parks, D. M. and Wang, Y.-Y. (1988), in *Analytical, Numerical and Experimental Aspects of Three Dimensional Fracture Processes*, ASME, AMD-91, Eds. A. J. Rosakis et al., ASME New York, pp. 19-32.

[5] Parks, D. M. (1991), in *Defect Assessment in Components - Fundamentals and Applications*, ESIS/EGF9, ed. by J.G. Blauel and K.-H. Schwalbe, Mechanical Engineering Publications, London, pp. 205-231.

[6] Parks, D. M. (1992), in *Topics of Fracture and Fatigue*, Edited by A. S. Argon, Springer Verlag New York, pp. 59-98.

[7] Al-Ani, A. M. and Hancock, J. W. (1991), *Journal of the Mechanics and Physics of Solids*, 39, pp. 23-43.

[8] Betegón, C. and Hancock, J. W. (1991), *Journal of Applied Mechanics*, 58, pp. 104-110.

[9] O'Dowd, N. P. and Shih, C. F. (1991), *Journal of the Mechanics and Physics of Solids*, 39, pp. 989-1015.

[10] O'Dowd, N. P. and Shih, C. F. (1992), *Journal of the Mechanics and Physics of Solids*, 40, pp. 939-963.

[11] Rice, J. R. (1968), *Journal of Applied Mechanics*, 35, pp. 379-386.

[12] Brocks, W. and Schmitt, W. (1993), "The second parameter in J-R curves: Constraint or triaxiality?" Presented on Second Symposium on Constraint Effects in Fracture, American Society for Testing and Materials, Fort Worth, Texas, USA, Nov. 17-18, 1993. To appear in ASTM STP.

[13] Williams, M. L. (1957), *Journal of Applied Mechanics*, 24, pp. 111-114.

[14] Yuan, H. (1994), "Discussions of constraint effects in crack front fields in elastoplastic materials", to be submitted for publication.

[15] ABAQUS User Manual, Version 5.2, Hibbitt, Karlsson & Sorensen, Inc., Providence, R. I. (1992)

[16] Yuan, H., et al. (1993), "Effects of loading biaxiality on plane stress crack-tip fields", *Engineering Fracture Mechanics*, to appear.

[17] Shih, C. F. and O'Dowd, N. P. (1993), "A fracture mechanics approach based on a toughness locus", presented on *International Conference Shallow Crack Fracture Mechanics, Toughness Tests and Applications*, Cambridge, UK, Sept. 1992.

[18] Shih, C. F., O'Dowd, N. P. and Kirk, M. T. (1993), in *Constraint Effects in Fracture, ASTM STP 1171*, American Society for Testing and Materials, Philadelphia, pp. 2-20.

[19] Yuan, H. and Lin, G. (1993), *International Journal of Fracture*, 61, pp.295-330.

[20] Yuan, H., et al. (1993), "Quantification of crack constraint effects in an austenitic steel", *International Journal of Fracture*, to appear.

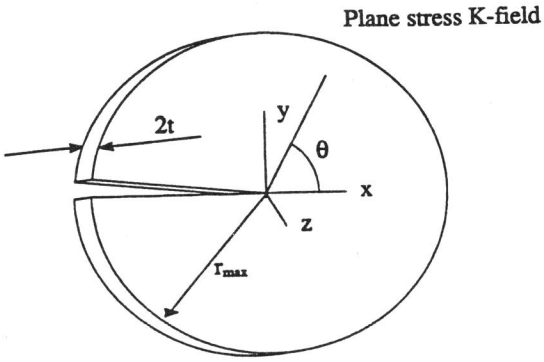

Fig. 1: Modified three-dimensional boundary layer formulation (MBLF)

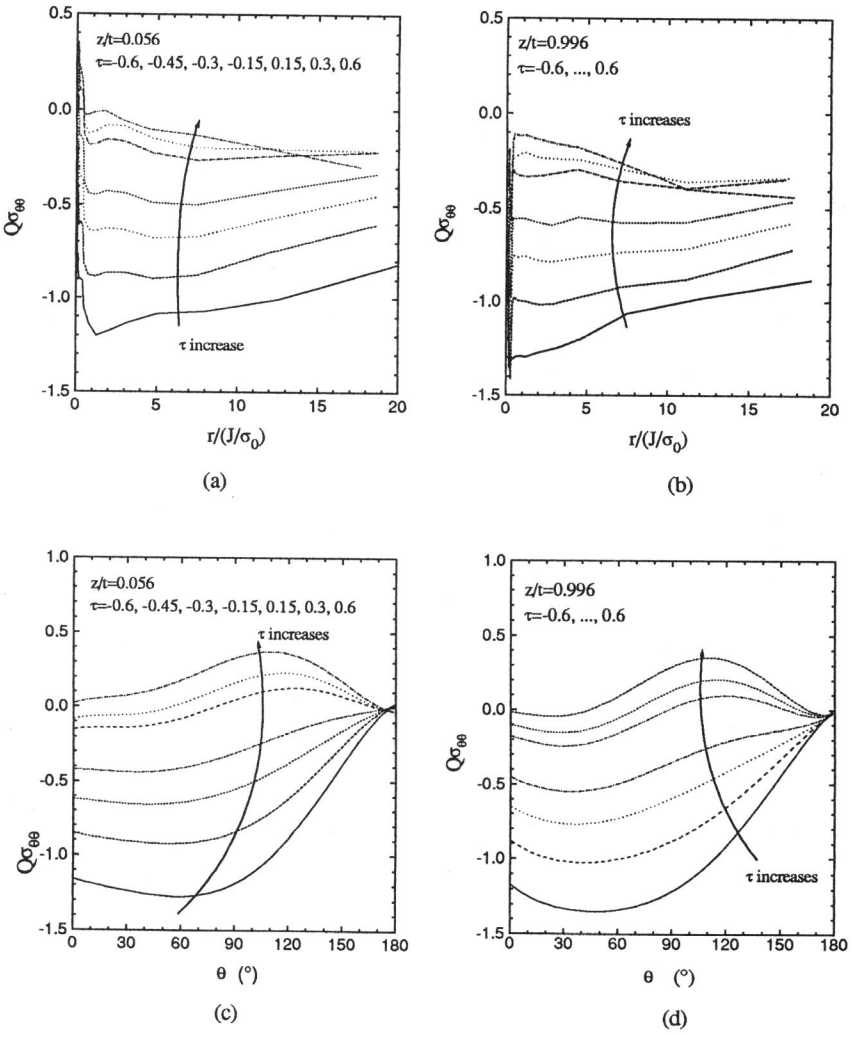

Fig. 2: Variations of the second term of the hoop stress with very small-scale yielding $r_p/t<0.1$.
(a) $\sigma_{\theta\theta}$-$r/(J/\sigma_0)$ at z/t=0.056; (b) $\sigma_{\theta\theta}$ - $r/(J/\sigma_0)$ at z/t=0.996; (c) $\sigma_{\theta\theta}$ - θ at z/t=0.056;
(d) $\sigma_{\theta\theta}$ - θ at z/t=0.996.

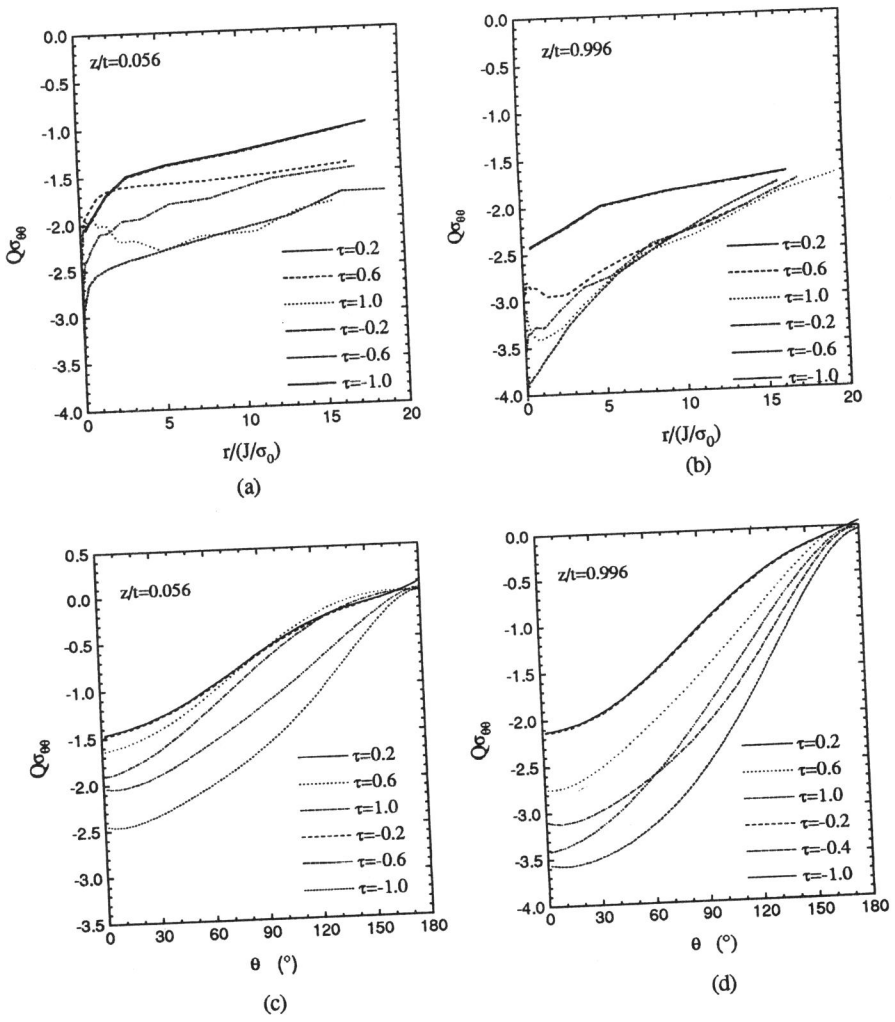

Fig. 3: Variations of the hoop stress with plastic zone sizes corresponding the plate thickness(r_p/t>0.5). (a) $\sigma_{\theta\theta}$ - r/(J/σ_0) at z/t=0.056; (b) $\sigma_{\theta\theta}$ - r/(J/σ_0) at z/t=0.996; (c) $\sigma_{\theta\theta}$ - θ at z/t=0.056; $\sigma_{\theta\theta}$ - θ at z/t=0.996.

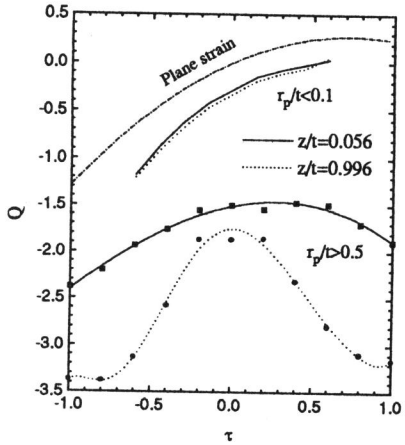

Fig. 4: Q as a function of the transverse stress τ. The plane strain results was reported in [17].

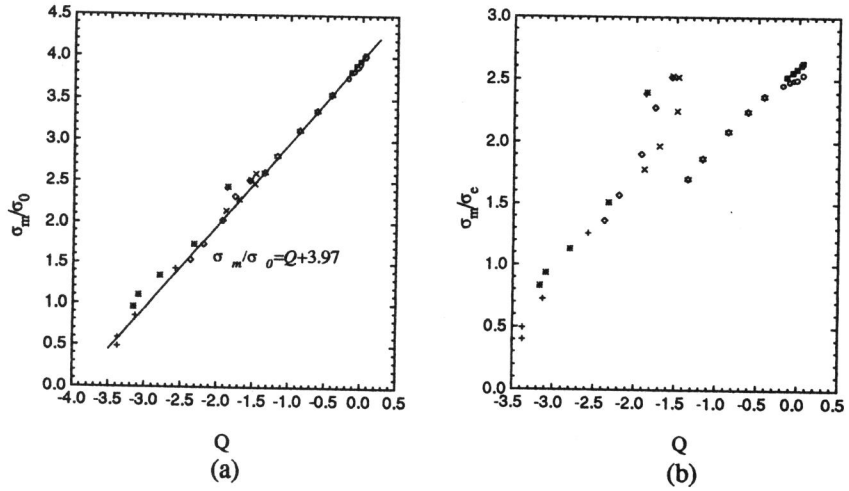

Fig. 5: Characterisation of the stress triaxiality at the crack tip ($r/(J/\sigma_0)=2$, $\theta=0$). The symbols denote the FE results under different biaxial loads at z=0.056 and 0.996, respectively. (a) Q - σ_m/σ_0; (b) Q - σ_m/σ_e.